

$\bar{D}N$ interaction in a color-confining chiral quark model

C. E. Fontoura, G. Krein, and V. E. Vizcarra

*Instituto de Física Teórica, Universidade Estadual Paulista**Rua Doutor Bento Teobaldo Ferraz, 271 - Bloco II, 01140-070 São Paulo, São Paulo, Brazil*

(Received 25 August 2012; revised manuscript received 23 October 2012; published 27 February 2013)

We investigate the low-energy elastic $\bar{D}N$ interaction using a quark model that confines color and realizes dynamical chiral symmetry breaking. The model is defined by a microscopic Hamiltonian inspired in the QCD Hamiltonian in Coulomb gauge. Constituent quark masses are obtained by solving a gap equation, and baryon and meson bound-state wave functions are obtained using a variational method. We derive a low-energy meson-nucleon potential from a quark-interchange mechanism whose ingredients are the quark-quark and quark-antiquark interactions and baryon and meson wave functions, all derived from the same microscopic Hamiltonian. The model is supplemented with $(\sigma, \rho, \omega, a_0)$ single-meson exchanges to describe the long-range part of the interaction. Cross sections and phase shifts are obtained by iterating the quark-interchange plus meson-exchange potentials in a Lippmann-Schwinger equation. Once coupling constants of long-range scalar σ and a_0 meson exchanges are adjusted to describe experimental phase shifts of the K^+N and K^0N reactions, predictions for cross sections and s -wave phase shifts for the \bar{D}^0N and D^-N reactions are obtained without introducing new parameters.

DOI: [10.1103/PhysRevC.87.025206](https://doi.org/10.1103/PhysRevC.87.025206)

PACS number(s): 21.30.Fe, 12.39.-x, 13.75.Cs

I. INTRODUCTION

The interaction of heavy-flavored hadrons with ordinary hadrons like nucleons and light mesons is focus of great contemporary interest in different contexts. One focus of interest is in experiments of relativistic heavy ion collisions. In heavy ion experiments, charm and bottom quarks are produced in the initial stages of the collision by hard scattering processes. Since they are much heavier than the light partons making up the bulk of the matter produced in the collision, it is likely that they will not equilibrate with the surrounding matter and therefore they might be ideal probes of properties of the expanding medium; for a recent review on the subject and an extensive list of references, see Ref. [1]. However, the heavy quarks will eventually hadronize and information on the medium will be carried out of the system by heavy-flavored hadrons. In their way out of the system, the heavy-flavored hadrons will interact with the more abundant light-flavored hadrons, and a good understanding of the interaction is crucial for a reliable interpretation of experimental data. Another focus of interest is an exciting physics program that will be carried out with the 12 GeV upgrade of the Continuous Electron Beam Facility (CEBAF) accelerator at the Jefferson Laboratory in the USA and the construction of the Facility for Antiproton and Ion Research (FAIR) facility in Germany. At the Jefferson Laboratory charmed hadrons will be produced by scattering electrons off nuclei and at FAIR they will be produced by the annihilation of antiprotons on nuclei. One particularly exciting perspective is the possibility of creating exotic nuclear bound states by nuclei capturing charmonia states like J/Ψ and η_c [2–5] or heavy-light D and D^* mesons [6–8]. In addition, the quest for experimental signals of chiral symmetry restoration in matter is a subject of immense current interest and open-charm D and D^* mesons are expected to play an important role in this respect; for a recent review, see Ref. [9]. In D mesons, properties of the light constituent quarks determined by dynamical chiral symmetry breaking

($D\chi$ SB), like masses and magnetic moments, are sensitive to the surrounding environment, and changes in those properties will impact the structure and interactions of the mesons in medium. Evidently, a prerequisite for reliable predictions of modifications of hadron properties in medium is a good understanding of the free-space interaction of these hadrons. Knowledge of the interaction in free space is also essential for guiding future experiments aiming at producing exotic bound states and measuring in-medium hadron properties.

The present paper is concerned with the low-energy interaction of $\bar{D} = (\bar{D}^0, D^-)$ mesons with nucleons in free space. There is a complete lack of experimental information on this reaction; all of what is presently known about the interaction in free space has been apprehended from model calculations based on hadronic Lagrangians motivated by flavor SU(4) symmetry [10–12], models using hadron and quark degrees of freedom [13] and heavy-quark symmetry [14,15], and the nonrelativistic quark model [16]. Although the first lattice QCD studies of the interaction of charmed hadrons like J/Ψ and η_c with nucleons are starting to appear in the literature [17–19], the $\bar{D}N$ interaction does not seem to have been considered by the lattice community. In view of this situation, the use of models seems to be the only alternative for making the urgently needed predictions for, e.g., low-energy cross sections of reactions involving charmed hadrons. However, as advocated in the works of Refs. [13,20–22], minimally reliable predictions of unknown cross sections need to be founded on models constrained as much as possible by symmetry arguments, analogies with other similar processes, and the use of different degrees of freedom. In the specific case of the $\bar{D}N$ reaction, Ref. [13] extended a very successful model for the KN reaction [23], in which the long-range part of the interaction is described within a meson-exchange framework [24,25] and the short-distance part is described by a quark-interchange mechanism from one-gluon exchange (OGE) of a nonrelativistic quark model (NRQM) [26–31].

The model of Ref. [23] describes the available low-energy experimental data for the KN reaction and was used to set limits on the width of the hypothetical $\Theta^+(1540)$ pentaquark state [32]. For the $\bar{D}N$ reaction, the model predicts cross sections that are on average of the same order of magnitude but larger by a factor roughly equal to 2 than those of the analogous K^+N and K^0N reactions for center-of-mass kinetic energies up to 150 MeV. Two interesting findings of the study of Ref. [13] are noteworthy: (1) quark interchange contributes about the same amount as meson exchanges to the $\bar{D}N$ s -wave phase shifts and (2) among the meson exchanges processes, scalar (σ) and vector (ω, ρ) are the most important contributors: Single Λ_c, Σ_c baryon-exchange diagrams and higher-order box diagrams involving $\bar{D}^*N, \bar{D}\Delta,$ and $\bar{D}^*\Delta$ intermediate states contribute very little. Recall that single-pion exchange is absent in this reaction. The same model was also used to examine the possibility of extracting information on the DN and $\bar{D}N$ interactions in an antiproton annihilation on the deuteron [20].

The fact that quark-interchange plays a prominent role in the $\bar{D}N$ reaction is very significant to the quest of experimental signals of chiral symmetry restoration via changes in the interactions of \bar{D} mesons in matter. As said, such changes would be driven at the microscopic level by modifications of the properties of the light u and d constituent quarks. However, within a NRQM there is no direct way to link $D\chi$ SB in medium and the effective hadron-hadron interactions, since constituent quark masses and microscopic interactions at the quark level are specified independently in the model [33]. Also, any temperature or density dependence on constituent quark masses has to be postulated in an *ad hoc* manner [34,35] to account for effects of $D\chi$ SB restoration. As a step to remedy this limitation of the NRQM, in the present paper we use a model that realizes $D\chi$ SB in a way that the same microscopic interaction that drives $D\chi$ SB also confines the quarks and antiquarks into color singlet hadronic states and in addition is the source of the hadron-hadron interaction. The model is defined by a microscopic Hamiltonian inspired in the QCD Hamiltonian in Coulomb gauge, in that an infrared divergent interaction models the full non-Abelian color Coulomb kernel in QCD and leads to hadron bound states that are color singlets. The Hamiltonian also contains an infrared finite interaction to model transverse-gluon interactions and leads to, among other effects, hyperfine splittings of hadron masses [36–38]. We implement an approximation scheme that allows calculation with little computational effort of variational hadron wave functions and effective hadron-hadron interactions that can be iterated in a Lippmann-Schwinger equation to calculate phase shifts and cross sections. An early calculation of the KN interaction within such a model, but using a confining interaction only, was performed in Ref. [39].

The paper is organized as follows. In the next section we present the microscopic quark-antiquark Hamiltonian of the model. We discuss $D\chi$ SB in the context of two models for the infrared divergent potentials that mimic the full non-Abelian color Coulomb kernel in QCD and obtain numerical solutions of the constituent quark mass function for different current quark masses. In Sec. III we discuss a calculation scheme for deriving effective low-energy hadron-hadron interactions

within the context of the Hamiltonian of the model. A low-momentum expansion of the quark mass function is used to obtain variational meson and baryon wave functions and explicit, analytical expressions for the effective meson-baryon potential. In Sec. IV we present numerical results for phase shifts and cross sections for the $K^+N, K^0N, \bar{D}^0N,$ and D^-N reactions at low energies. Initially we use the short-ranged quark-interchange potential derived within the model and add potentials from one-meson exchanges to fit experimental s -wave phase shifts of the K^+N and K^0N reactions. Next, without introducing new parameters, we present the predictions of the model for the \bar{D}^0N and D^-N reactions. Our conclusions and perspectives are presented in Sec. V. The paper includes one appendix that presents the meson Lagrangians and respective one-meson exchange potentials.

II. MICROSCOPIC HAMILTONIAN AND THE CONSTITUENT QUARK MASS FUNCTION

The Hamiltonian of the model is given as

$$H = H_0 + H_{\text{int}}, \quad (1)$$

where H_0 and H_{int} are given in terms of a quark field operator $\Psi(\mathbf{x})$ as

$$H_0 = \int d\mathbf{x} \Psi^\dagger(\mathbf{x})(-i\boldsymbol{\alpha} \cdot \nabla + \beta m)\Psi(\mathbf{x}) \quad (2)$$

and

$$H_{\text{int}} = -\frac{1}{2} \int d\mathbf{x} d\mathbf{y} \rho^a(\mathbf{x}) V_C(|\mathbf{x} - \mathbf{y}|) \rho^a(\mathbf{y}) + \frac{1}{2} \int d\mathbf{x} d\mathbf{y} J_i^a(\mathbf{x}) D^{ij}(|\mathbf{x} - \mathbf{y}|) J_j^a(\mathbf{y}). \quad (3)$$

In the above, m is the current-quark mass matrix of the light $l = (u, d)$, strange s , and charm c quarks:

$$m = \begin{pmatrix} m_u & 0 & 0 & 0 \\ 0 & m_d & 0 & 0 \\ 0 & 0 & m_s & 0 \\ 0 & 0 & 0 & m_c \end{pmatrix}, \quad (4)$$

$\rho^a(\mathbf{x})$ is the color charge density

$$\rho^a(\mathbf{x}) = \Psi^\dagger(\mathbf{x}) T^a \Psi(\mathbf{x}), \quad (5)$$

and $J_i^a(\mathbf{x})$ is the color current density

$$J_i^a(\mathbf{x}) = \Psi^\dagger(\mathbf{x}) T^a \alpha_i \Psi(\mathbf{x}), \quad (6)$$

with $T^a = \lambda^a/2$, where λ^a are the SU(3) Gell-Mann matrices. V_C and D^{ij} are the effective Coulomb and transverse-gluon interactions; the transversity of D^{ij} implies

$$D^{ij}(|\mathbf{x} - \mathbf{y}|) = \left(\delta^{ij} - \frac{\nabla^i \nabla^j}{\nabla^2} \right) D_T(|\mathbf{x} - \mathbf{y}|). \quad (7)$$

The problem of $D\chi$ SB with such an Hamiltonian has been discussed in the literature for a long time in Bardeen-Cooper-Schrieffer (BCS) mean-field-type approaches via

Bogoliubov-Valatin transformations or Dyson-Schwinger equations in the rainbow approximation [40–54]. For our purposes in the present paper, it is more convenient to follow the logic of the Bogoliubov-Valatin transformations. In this approach, $D\chi$ SB is characterized by a momentum-dependent *constituent-quark* mass function $M(k)$, so that the quark field operator of a given color and flavor can be expanded as

$$\Psi(\mathbf{x}) = \sum_s \int \frac{d\mathbf{k}}{(2\pi)^3} [u_s(\mathbf{k})q_s(\mathbf{k}) + v_s(\mathbf{k})\bar{q}_s^\dagger(-\mathbf{k})]e^{i\mathbf{k}\cdot\mathbf{x}}, \quad (8)$$

where $u_s(\mathbf{k})$ and $v_s(\mathbf{k})$ are Dirac spinors:

$$u_s(\mathbf{k}) = \sqrt{\frac{E(k) + M(k)}{2E(k)}} \begin{pmatrix} 1 \\ \frac{\boldsymbol{\sigma}\cdot\mathbf{k}}{E(k)+M(k)} \end{pmatrix} \chi_s, \quad (9)$$

$$v_s(\mathbf{k}) = \sqrt{\frac{E(k) + M(k)}{2E(k)}} \begin{pmatrix} -\frac{\boldsymbol{\sigma}\cdot\mathbf{k}}{E(k)+M(k)} \\ 1 \end{pmatrix} \chi_s^c, \quad (10)$$

with $E(k) = [k^2 + M^2(k)]^{1/2}$, χ_s is a Pauli spinor, $\chi_s^c = -i\sigma^2\chi_s^*$, and $q_s^\dagger(\mathbf{k})$, $\bar{q}_s^\dagger(\mathbf{k})$, $q_s(\mathbf{k})$, and $\bar{q}_s(\mathbf{k})$ are creation and annihilation operators of *constituent quarks*; $q_s(\mathbf{k})$ and $\bar{q}_s(\mathbf{k})$ annihilate the vacuum state $|\Omega\rangle$:

$$q_s(\mathbf{k})|\Omega\rangle = 0, \quad \bar{q}_s(\mathbf{k})|\Omega\rangle = 0. \quad (11)$$

For $m = 0$, the Hamiltonian is chirally symmetric, but $|\Omega\rangle$ is not symmetric, $\langle\Omega|\bar{\Psi}\Psi|\Omega\rangle \neq 0$.

By substituting in Eqs. (2) and (3) the expansion of Ψ , Eq. (8) and rewriting H in Wick-contracted form, one obtains an expression for H that can be written as a sum of three parts:

$$H = \mathcal{E} + H_2 + H_4, \quad (12)$$

where \mathcal{E} is the c -number vacuum energy and H_2 and H_4 are normal-ordered operators, respectively, quadratic and quartic in the creation and annihilation operators. The mass function $M(k)$ is determined by demanding that H_2 is diagonal in the quark operators. This leads to the *gap equation* for the constituent quark mass function $M_f(k)$ of flavor f :

$$M_f(k) = m_f + \frac{2}{3} \int \frac{d\mathbf{q}}{(2\pi)^3} [F_f^{(1)}(\mathbf{k}, \mathbf{q}) V_C(|\mathbf{k} - \mathbf{q}|) + 2G_f^{(1)}(\mathbf{k}, \mathbf{q}) D_T(|\mathbf{k} - \mathbf{q}|)], \quad (13)$$

where m_f is the current quark mass and

$$F_f^{(1)}(\mathbf{k}, \mathbf{q}) = \frac{M_f(q)}{E_f(q)} - \frac{M_f(k)}{E_f(k)} \frac{q}{k} \hat{\mathbf{k}} \cdot \hat{\mathbf{q}}, \quad (14)$$

$$G_f^{(1)}(\mathbf{k}, \mathbf{q}) = \frac{M_f(q)}{E_f(q)} + \frac{M_f(k)}{E_f(k)} \frac{q}{k} \times \frac{(\mathbf{k} \cdot \mathbf{q} - k^2)(\mathbf{k} \cdot \mathbf{q} - q^2)}{kq|\mathbf{k} - \mathbf{q}|^2}, \quad (15)$$

and $V_C(k)$ and $D_T(k)$ are the Fourier transforms of $V_C(|\mathbf{x}|)$ and $D_T(|\mathbf{x}|)$. The quadratic Hamiltonian H_2 is given by

$$H_2 = \sum_{s,f} \int d\mathbf{k} \varepsilon_f(k) [q_{sf}^\dagger(\mathbf{k})q_{sf}(\mathbf{k}) + \bar{q}_{sf}^\dagger(\mathbf{k})\bar{q}_{sf}(\mathbf{k})], \quad (16)$$

where $\varepsilon_f(k)$ is the constituent-quark single-particle energy of flavor f , given by

$$\varepsilon_f(k) = \frac{k^2 + m_f M_f(k)}{E_f(k)} + \frac{2}{3} \int \frac{d\mathbf{q}}{(2\pi)^3} [F_f^{(2)}(\mathbf{k}, \mathbf{q}) V_C(|\mathbf{k} - \mathbf{q}|) + 2G_f^{(2)}(\mathbf{k}, \mathbf{q}) D_T(|\mathbf{k} - \mathbf{q}|)], \quad (17)$$

with

$$F_f^{(2)}(\mathbf{k}, \mathbf{q}) = \frac{M_f(k)}{E_f(k)} \frac{M_f(q)}{E_f(q)} + \frac{\mathbf{k} \cdot \mathbf{q}}{E_f(k)E_f(q)} \quad (18)$$

and

$$G_f^{(2)}(\mathbf{k}, \mathbf{q}) = \frac{M_f(k)}{E_f(k)} \frac{M_f(q)}{E_f(q)} + \frac{(\mathbf{k} \cdot \mathbf{q} - k^2)(\mathbf{k} \cdot \mathbf{q} - q^2)}{E_f(k)E_f(q)|\mathbf{k} - \mathbf{q}|^2}. \quad (19)$$

The four-fermion term H_4 is simply the normal-ordered form of H_{int} :

$$H_4 = : H_{\text{int}} : . \quad (20)$$

The color-confining feature of the Hamiltonian is discussed in the next section.

To solve the gap equation one needs to specify the interactions V_C and D_T . For the confining Coulomb term V_C , we use two analytical forms, model 1 and model 2, to assess the sensitivity of results with respect to V_C . Model 1 is a parametrization of the lattice simulation of QCD in Coulomb gauge of Ref. [55]:

$$V_C(k) = \frac{8\pi\sigma_{\text{Coul}}}{k^4} + \frac{4\pi C}{k^2}, \quad (21)$$

with $\sigma_{\text{Coul}} = (552 \text{ MeV})^2$ and $C = 6$. Model 2 for V_C was used in recent studies of glueballs [56] and heavy hybrid quarkonia [57]; it is written as

$$V_C(k) = V_l(k) + V_s(k), \quad (22)$$

where

$$V_l(k) = \frac{8\pi\sigma}{k^4}, \quad V_s(k) = \frac{4\pi\alpha(k)}{k^2}, \quad (23)$$

with

$$\alpha(k) = \frac{4\pi Z}{\beta^{3/2} \ln^{3/2}(c + k^2/\Lambda_{\text{QCD}}^2)}. \quad (24)$$

The parameters here are $\Lambda_{\text{QCD}} = 250 \text{ MeV}$, $Z = 5.94$, $c = 40.68$, and $\beta = 121/12$. For the transverse-gluon interaction D_T we use

$$D_T(k) = -\frac{4\pi\alpha_T}{(k^2 + m^2) \ln^{1.42}(\tau + k^2/m_g^2)}. \quad (25)$$

This choice is guided by previous studies of spin-hyperfine splittings of meson masses [38] using a Hamiltonian as in the present work. Moreover, the Yukawa term multiplying the log term is to model lattice results [55,58] that indicate that the gluon propagator in Coulomb gauge is finite at $k^2 = 0$, i.e., not divergent like the free propagator $1/k^2$. Further ahead we discuss the impact of this particular choice of infrared behavior

on our numerical results. Parameters here are $m_g = 550$ MeV, $m = m_g/2$, $\tau = 1.05$, and $\alpha_T = 0.5$. We use the same D_T for both models. We note that we could have used a log running similar to the one in V_C , Eq. (24), but results would not change in any significant way.

We have solved the gap equation in Eq. (13) by iteration. The angular integrals can be performed analytically, but special care must be taken with the strongly peaked confining term $1/|\mathbf{k} - \mathbf{q}|^4$ at $\mathbf{q} \approx \mathbf{k}$ in the numerical integration over q . There is no actual divergence here: the terms $M(q)/E(q)$ and $M(k)/E(q)(q/k)\hat{\mathbf{k}} \cdot \hat{\mathbf{q}}$ in Eq. (14) cancel exactly when $\mathbf{q} = \mathbf{k}$, but this cancellation can be problematic in the numerical integration. This problem can be handled in different manners, like via the use of a momentum mesh containing node and half-node points with, e.g., k at nodes and q at half-nodes [44], or via the introduction of a mass parameter μ_{ir} such $k^4 \rightarrow (k^2 + \mu^2)^2$ in Eq. (21) and varying μ_{ir} until results become independent of μ_{ir} [59]. In the present paper we use a different method [60]; we add a convenient zero to the gap equation:

$$-\int \frac{d\mathbf{q}}{(2\pi)^3} \frac{1}{|\mathbf{k} - \mathbf{q}|^4} \frac{M(k)}{E(k)} \frac{1}{k} \hat{\mathbf{k}} \cdot (\mathbf{k} - \mathbf{q}), \quad (26)$$

and rewrite $F^{(1)}(\mathbf{k}, \mathbf{q})$ in Eq. (13) as

$$\begin{aligned} F^{(1)}(\mathbf{k}, \mathbf{q}) &\rightarrow F^{(1)}(\mathbf{k}, \mathbf{q}) - \frac{M(k)}{E(k)} \frac{1}{k} \hat{\mathbf{k}} \cdot (\mathbf{k} - \mathbf{q}) \\ &= \left(\frac{M(q)}{E(q)} - \frac{M(k)}{E(k)} \right) \\ &\quad - \left(\frac{q}{k} \hat{\mathbf{k}} \cdot \hat{\mathbf{q}} - 1 \right) \left(\frac{M(k)}{E(q)} - \frac{M(k)}{E(k)} \right), \quad (27) \end{aligned}$$

so that angle-independent and angle-dependent terms vanish independently when $\mathbf{q} = \mathbf{k}$. This feature makes the numerical cancellation of the divergences very stable.

In Fig. 1 we present solutions $M(k)$ of the gap equation for different values of current-quark masses. The dramatic effect of $D\chi$ SB mass generation is seen clearly in the figure: for the fictitious limit of a zero current-quark mass (solid line), the mass function $M(k)$ acquires a sizable value in the infrared, $M(k=0) \approx 250$ MeV. In the ultraviolet, the mass function runs logarithmically with k , in a manner dictated by the running of the microscopic interactions. Since the model interactions used here have a different ultraviolet running from the one dictated by perturbative QCD, the logarithm running of the quark-mass function must be different; the interactions here fall off faster than those in QCD. One consequence of this is that the momentum integral over the trace of the quark propagator, which gives the quark condensate, does not run and is ultraviolet finite in the present case; we obtain $(-\langle \bar{\Psi}\Psi \rangle)^{1/3} = 280$ MeV. For nonzero current-quark masses, Fig. 1 shows that the effect of mass generation diminishes as the value of m_f increases: Here $m_u = m_d = 10$ MeV, $m_s = 150$ MeV in both models, and $m_c = 950$ MeV in model 1 and $m_c = 600$ MeV in model 2. On the logarithm scale, one sees that the mass function varies substantially in the ultraviolet, from $k \simeq 3\Lambda_{\text{QCD}} = 750$ MeV onward. It is worth noticing that although the momentum dependence of the mass function of the charm quark is much less dramatic than of

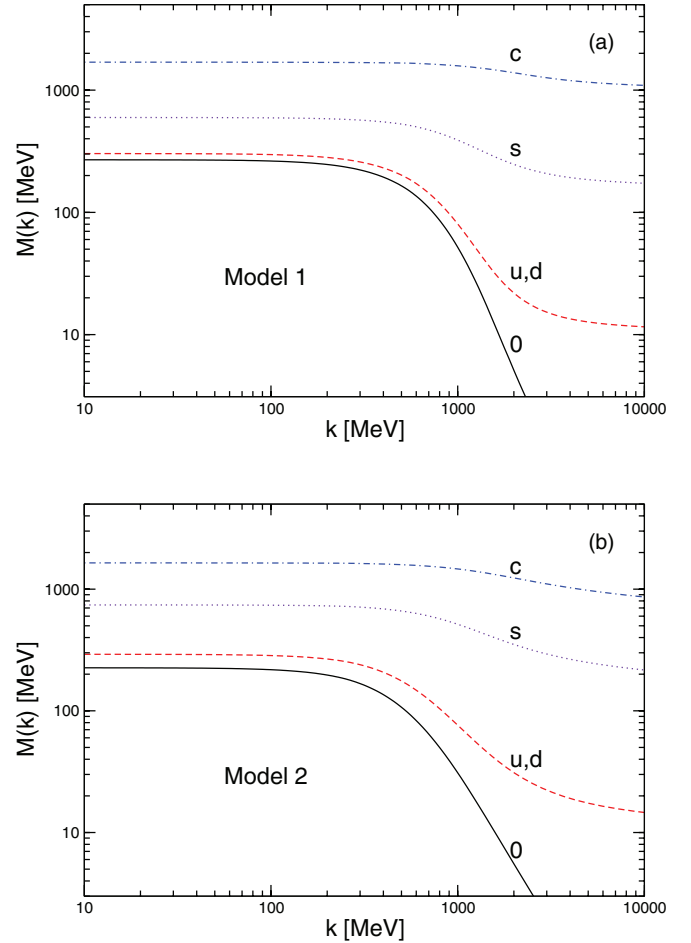


FIG. 1. (Color online) Constituent quark mass $M(k)$ as a function of the momentum for different values of current-quark masses.

the corresponding for light quarks, there is still a significant dressing effect, $M_c(0)/m_c \sim 1.5\text{--}3$, similarly to what is found with covariant Dyson-Schwinger equations [61–63].

Finally, we comment on the impact of the momentum dependence of $D_T(k)$ in the infrared on the mass function. In the absence of D_T , using only V_C with the parameters above, $M(0)$ would be of the order of 100 MeV in the chiral limit. On the other hand, using a $D_T(k)$ that vanishes at $k = 0$, like in the form of a Gribov formula [64], would give $M(0) \sim 200$ MeV in the chiral limit. This is in line with the recent finding of Ref. [65], which studies $D\chi$ SB in a framework based on a quark wave functional determined by the variational principle using an ansatz that goes beyond the BCS-type of wave functionals.

III. BARYON-MESON INTERACTION

In this section we set up a calculation for deriving effective low-energy hadron-hadron interactions with the Hamiltonian discussed above. We seek a scheme that makes contact with traditional quark-model calculations and can be systematically improved with some computational effort. Since the early 1980s, the great majority of calculations of hadron-hadron

scattering observables in the quark model are based on methods to handle cluster dynamics adapted from nuclear or atomic physics; for reviews on methodology and fairly complete lists of references, see Refs. [66–68]. Such methods require a microscopic Hamiltonian and hadron bound-state wave functions given in terms of quark degrees of freedom. Within the context of the model discussed in the previous section, the starting point is the microscopic Hamiltonian of Eq. (1), with quark field operators given in terms of the constituent quark mass function $M(k)$ obtained from the numerical solution of the gap equation in Eq. (13).

The sector of the Hamiltonian relevant for the elastic meson-baryon interaction can be written in a compact notation as

$$H_{q\bar{q}} = \varepsilon(\mu) q_{\mu}^{\dagger} q_{\mu} + \varepsilon(\nu) \bar{q}_{\nu}^{\dagger} \bar{q}_{\nu} + \frac{1}{2} V_{qq}(\mu\nu; \sigma\rho) q_{\mu}^{\dagger} q_{\nu}^{\dagger} q_{\rho} q_{\sigma} + \frac{1}{2} V_{q\bar{q}}(\mu\nu; \sigma\rho) \bar{q}_{\mu}^{\dagger} \bar{q}_{\nu}^{\dagger} \bar{q}_{\rho} \bar{q}_{\sigma} + V_{q\bar{q}}(\mu\nu; \sigma\rho) q_{\mu}^{\dagger} \bar{q}_{\nu}^{\dagger} \bar{q}_{\rho} q_{\sigma}, \quad (28)$$

where the indices $\mu, \nu, \rho,$ and σ denote collectively the quantum numbers (orbital, color, spin, flavor) of quarks and antiquarks. The first two terms in Eq. (28) are the quark and antiquark single-particle self-energies coming from Eq. (16), and $V_{qq}, V_{q\bar{q}},$ and $V_{\bar{q}\bar{q}}$ are respectively the quark-quark, quark-antiquark, and antiquark-antiquark interactions from H_4 in Eq. (20). The one-baryon state in the BCS approximation can be written in the schematic notation as [47,51,52]

$$|a\rangle = B_a^{\dagger} |\Omega\rangle = \frac{1}{\sqrt{3!}} \psi_a^{\mu_1\mu_2\mu_3} q_{\mu_1}^{\dagger} q_{\mu_2}^{\dagger} q_{\mu_3}^{\dagger} |\Omega\rangle, \quad (29)$$

with $\psi_a^{\mu_1\mu_2\mu_3}$ being the Fock-space amplitude, with a denoting the (orbital, spin, flavor) quantum numbers of the baryon. Likewise, the one-meson state is written as

$$|a\rangle = M_a^{\dagger} |\Omega\rangle = \phi_a^{\mu\nu} q_{\mu}^{\dagger} \bar{q}_{\nu}^{\dagger} |\Omega\rangle, \quad (30)$$

where $\phi_a^{\mu\nu}$ is the corresponding Fock-space amplitude, with a representing the quantum numbers of the meson. The Fock-space amplitudes ψ and ϕ can be obtained by solving a Salpeter-type equation [47,51,52].

Given a microscopic Hamiltonian $H_{q\bar{q}}$ and hadronic states $|a\rangle$ as in Eqs. (28)–(30), an effective low-energy meson-baryon potential for the process Meson(a) + Baryon(b) \rightarrow Meson(c) + Baryon(d), $V_{MB}(ab, cd)$, can be written as [67]

$$V_{MB}(ab, cd) = -3 \phi_c^{*\mu\nu_1} \psi_d^{*\nu_1\mu_2\mu_3} V_{qq}(\mu\nu; \sigma\rho) \phi_a^{\rho\nu_1} \psi_b^{\sigma\mu_2\mu_3} - 3 \phi_c^{*\sigma\rho} \psi_d^{*\mu_1\mu_2\mu_3} V_{q\bar{q}}(\mu\nu; \sigma\rho) \phi_a^{\mu_1\rho} \psi_b^{\mu_2\mu_3} - 6 \phi_c^{*\mu_1\nu_1} \psi_d^{*\nu_1\mu_2\mu_3} V_{qq}(\mu\nu; \sigma\rho) \phi_a^{\rho\nu_1} \psi_b^{\mu_1\sigma\mu_3} - 6 \phi_c^{*\nu_1\nu} \psi_d^{*\nu_1\mu_2\mu_3} V_{q\bar{q}}(\mu\nu; \sigma\rho) \phi_a^{\nu_1\rho} \psi_b^{\mu_1\sigma\mu_3}, \quad (31)$$

where $\phi_a^{\mu\nu}, \psi_b^{\mu\nu\sigma}, \dots,$ are the meson and baryon Fock-space amplitudes of Eqs. (29) and (30) and $V_{qq}, V_{q\bar{q}},$ and $V_{\bar{q}\bar{q}}$ are respectively the quark-quark, quark-antiquark, and antiquark-antiquark interactions in $H_{q\bar{q}}$ of Eq. (28). The expression in Eq. (31) is completely general, in that it is valid for any low-energy meson-baryon process for which the baryon and meson Fock-space states and $H_{q\bar{q}}$ are as given above. It can be iterated in a Lippmann-Schwinger equation to obtain scattering phase shifts and cross sections; for details, see

Ref. [67]. There is, however, one difficulty: V_{MB} involves multidimensional integrals over internal quark and antiquark momenta of products of baryon and meson wave functions and products of Dirac spinors $u(\mathbf{k})$ and $v(\mathbf{k})$ that depend on the quark mass function $M(k)$. Although this is not a major difficulty, an approximation can be made, noting that the bound-state amplitudes ψ and ϕ are expected to fall off very fast in momentum space for momenta larger than the inverse size of the hadron, and therefore only low-momentum quark and antiquark processes contribute in the multidimensional integrals. In view of this, and the fact that $M(k)$ changes considerably only at large momenta, a natural approximation scheme to simplify the calculations without sacrificing the low-energy content of the effective interaction is to retain the first few terms in the low-momentum expansion for the mass function $M(k)$:

$$M(k) = M + M'(0)k + \frac{1}{2}M''(0)k^2 + \dots, \quad (32)$$

where $M'(k) = dM(k)/dk$ and $M''(k) = d^2M(k)/dk^2$. In particular, by retaining terms up to $O(k^2/M^2)$ in the expansion, it is not difficult to show that the Dirac spinors $u_s(\mathbf{k})$ and $v_s(\mathbf{k})$ in Eqs. (9) and (10) become

$$u_s(\mathbf{k}) = \begin{pmatrix} 1 - \frac{k^2}{8M^2} \\ \frac{\sigma \cdot \mathbf{k}}{2M} \end{pmatrix} \chi_s, \quad (33)$$

$$v_s(\mathbf{k}) = \begin{pmatrix} -\frac{\sigma \cdot \mathbf{k}}{2M} \\ 1 - \frac{k^2}{8M^2} \end{pmatrix} \chi_s^c. \quad (34)$$

By using these spinors in Eq. (3), the expressions one obtains for $V_{qq}, V_{q\bar{q}},$ and $V_{\bar{q}\bar{q}}$ are very similar to those of the Fermi-Breit expansion of the OGE interaction [69]. There is, however, one important difference here: While for the OGE one has $V_C(k) = D_T(k) \approx 1/k^2$, in the present case $V_C(k)$ and $D_T(k)$ are different and represent very different physics; V_C is a confining interaction and D_T is a (static) transverse gluon interaction.

The evaluation of multidimensional integrals can be further simplified using the variational method of Refs. [47,51] with Gaussian ansatz for the bound-state amplitudes ψ and ϕ , instead of solving numerically Salpeter-type equations. Specifically,

$$\psi_{\mathbf{P}}(\mathbf{k}_1, \mathbf{k}_2, \mathbf{k}_3) = \delta(\mathbf{P} - \mathbf{k}_1 - \mathbf{k}_2 - \mathbf{k}_3) \times \left(\frac{3}{\pi^2 \alpha^4} \right)^{3/4} e^{-\sum_{i=1}^3 (\mathbf{k}_i - \mathbf{P}/3)/2\alpha^2}, \quad (35)$$

$$\phi_{\mathbf{P}}(\mathbf{k}_1, \mathbf{k}_2) = \delta(\mathbf{P} - \mathbf{k}_1 - \mathbf{k}_2) \times \left(\frac{1}{\pi \beta^2} \right)^{3/4} e^{-(M_1 \mathbf{k}_1 - M_2 \mathbf{k}_2)^2/8\beta^2}, \quad (36)$$

where α and β are variational parameters, \mathbf{P} is the center-of-mass momentum of the hadrons, and

$$M_1 = \frac{2M_{\bar{q}}}{(M_q + M_{\bar{q}})}, \quad M_2 = \frac{2M_q}{(M_q + M_{\bar{q}})}, \quad (37)$$

TABLE I. Variational size parameters of the hadron amplitudes and hadron mass differences. All values are in million electron volts.

	α	β_K	β_D	ΔM_{NK}	ΔM_{DN}	ΔM_{DK}
Model 1	568	425	508	350	990	1345
Model 2	484	364	423	205	1010	1220
OGE Refs. [13,23]	400	350	383.5			
Experiment				443	928	1371

with M_q and $M_{\bar{q}}$ being the zero-momentum constituent-quark masses. The variational parameters are determined by

$$\begin{aligned}
 M_N &= 3 \left(\frac{3}{\pi \alpha^2} \right)^{3/2} \int d\mathbf{k} \left[\frac{k^2}{E_l(k)} + m_l \frac{M_l(k)}{E_l(k)} \right] e^{-3k^2/\alpha^2} \\
 &+ \left(\frac{3}{2\pi \alpha^2} \right)^{3/2} \int \frac{d\mathbf{k}d\mathbf{q}}{(2\pi)^3} [2F_l^{(2)}(\mathbf{k}, \mathbf{q}) + 3C_N e^{-(\mathbf{k}-\mathbf{q})^2/2\alpha^2}] V_C(|\mathbf{k}-\mathbf{q}|) e^{-3k^2/2\alpha^2} \\
 &+ \left(\frac{3}{2\pi \alpha^2} \right)^{3/2} \int \frac{d\mathbf{k}d\mathbf{q}}{(2\pi)^3} \left[4G_l^{(2)}(\mathbf{k}, \mathbf{q}) - \frac{(\mathbf{k}-\mathbf{q})^2}{3M_l^2} e^{-(\mathbf{k}-\mathbf{q})^2/2\alpha^2} \right] D_T(|\mathbf{k}-\mathbf{q}|) e^{-k^2/\alpha^2}, \\
 M_P &= \left(\frac{1}{\pi \beta^2} \right)^{3/2} \int d\mathbf{k} \left[\frac{k^2}{E_l(k)} + m_l \frac{M_l(k)}{E_l(k)} + \frac{k^2}{E_h(k)} + m_h \frac{M_h(k)}{E_h(k)} \right] e^{-k^2/\beta^2} \\
 &+ \left(\frac{1}{\pi \beta^2} \right)^{3/2} \int \frac{d\mathbf{k}d\mathbf{q}}{(2\pi)^3} \left\{ \frac{2}{3} [F_l^{(2)}(\mathbf{k}, \mathbf{q}) + F_h^{(2)}(\mathbf{k}, \mathbf{q})] + C_P e^{-(\mathbf{k}-\mathbf{q})^2/2\beta^2} \right\} V_C(|\mathbf{k}-\mathbf{q}|) e^{-k^2/\beta^2} \\
 &+ \frac{4}{3} \left(\frac{1}{\pi \beta^2} \right)^{3/2} \int \frac{d\mathbf{k}d\mathbf{q}}{(2\pi)^3} \left[G_l^{(2)}(\mathbf{k}, \mathbf{q}) + G_h^{(2)}(\mathbf{k}, \mathbf{q}) + \frac{1}{2} \frac{(\mathbf{k}-\mathbf{q})^2}{M_l M_h} e^{-(\mathbf{k}-\mathbf{q})^2/2\beta^2} \right] D_T(|\mathbf{k}-\mathbf{q}|) e^{-k^2/\beta^2},
 \end{aligned} \tag{39}$$

where $F_{l,h}^{(2)}(\mathbf{k}, \mathbf{q})$ and $G_{l,h}^{(2)}(\mathbf{k}, \mathbf{q})$ are given in Eqs. (18) and (19) and the indices l and h refer to light and heavy flavors, $l = (u, d)$ and $h = (s, c)$. The matrix elements of the color matrices, $C_N = \langle N | T^a T^a | N \rangle$ and $C_P = \langle P | T^a (-T^a)^T | P \rangle$, in the terms proportional to the Coulomb potential V_C —that come from H_4 —are written to emphasize the color-confinement feature of the model [47]: For $\mathbf{k} = \mathbf{q}$, these terms are divergent, *unless* the color matrix elements are such that the corresponding expressions vanish. The terms $F_{l,h}^{(2)}(\mathbf{k}, \mathbf{q})$ come from H_2 , which is diagonal in color. For baryon and meson *color singlet states*, the contributions from H_2 and H_4 cancel exactly for $\mathbf{k} = \mathbf{q}$, since

$$C_N = \frac{\varepsilon^{c_1 c_2 c_3} \varepsilon^{c'_1 c'_2 c'_3}}{3!} (T^a)^{c_1 c'_1} (T^a)^{c_2 c'_2} = -\frac{2}{3}, \tag{41}$$

$$C_P = \frac{\delta^{c_1 c_2} \delta^{c'_1 c'_2}}{3} (T^a)^{c_1 c'_1} (-T^a)^{c_2 c'_2} = -\frac{4}{3}, \tag{42}$$

and

$$\lim_{\mathbf{k} \rightarrow \mathbf{q}} F_{l,h}^{(2)}(\mathbf{k}, \mathbf{q}) = 1. \tag{43}$$

Such a cancellation of infrared divergences also plays an important role in context of a conjectured [70] new high-density phase of matter composed of confined but chirally symmetric hadrons [71,72].

minimizing the hadron masses:

$$M_a = \frac{\langle a | (H_2 + H_4) | a' \rangle}{\langle a | a' \rangle} \Big|_{\mathbf{p}_a = \mathbf{p}_{a'} = 0}, \tag{38}$$

where we left out the constant \mathcal{E} , defined in Eq. (12), which cancels in the hadron mass differences (see Table I).

In this work we consider the elastic scattering of the pseudoscalar mesons (K^+ , K^0) and (\bar{D}^0 , D^-) off nucleons, with both the mesons and nucleons in their ground states. Using the Gaussian forms for the amplitudes ψ and ϕ , Eqs. (35) and (36), one obtains for the nucleon mass, M_N , and for the pseudoscalar meson mass, M_P , the following expressions:

Next, we obtain an explicit expression for the effective meson-nucleon interaction V_{MB} , given in a compact notation by Eq. (31). This effective interaction is generated by a quark-interchange mechanism. The use of Gaussian wave functions is very helpful for getting a V_{MB} in closed form [67]: It can be written as a sum of four contributions (see Eqs. (9) and (10) of Ref. [13]), each contribution corresponding to a quark-interchange diagram shown in Fig. 2:

$$V_{MB}(\mathbf{p}, \mathbf{p}') = \frac{1}{2} \sum_{i=1}^4 \omega_i [V_i(\mathbf{p}, \mathbf{p}') + V_i(\mathbf{p}', \mathbf{p})], \tag{44}$$

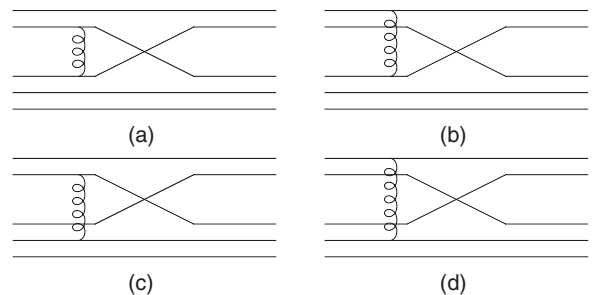


FIG. 2. Pictorial representation of the quark-interchange processes that contribute to a meson-baryon interaction. The curly lines represent the interactions V_C and D_T .

where \mathbf{p} and \mathbf{p}' are the initial and final center-of-mass momenta and the $V_i(\mathbf{p}, \mathbf{p}')$ are given by

$$V_i(\mathbf{p}, \mathbf{p}') = \left[\frac{3g}{(3 + 2g)\pi\alpha^2} \right] e^{-a_i p^2 - b_i p'^2 + c_i \mathbf{p} \cdot \mathbf{p}'} \times \int \frac{d\mathbf{q}}{(2\pi)^3} v(q) e^{-d_i q^2 + e_i \cdot \mathbf{q}}, \quad (45)$$

where the $a_i, b_i, c_i, d_i,$ and e_i involve the hadron sizes α and β and the constituent quark masses $M_u, M_s,$ and $M_c,$ and $g = (\alpha/\beta)^2$. Since we are using the same Fock-space amplitudes ψ and ϕ as those used in Ref. [13], the expressions for $a_i, b_i, \dots,$ are the same as there. It is important to note that the essential difference here as compared to Ref. [13] is that the constituent quark masses $M_u, M_s,$ and M_c ; the width parameters α and β ; and the meson-baryon interaction are all derived from the same microscopic quark-gluon Hamiltonian. Another very important difference here is $v(q)$: While in Ref. [13] it comes from the OGE, here $v(q) = V_C(q)$ for the spin-independent interaction and $v(q) = 2q^2/(3M_l M')$ $D_T(q)$ for the spin-spin interaction, with $M' = M_l$ for diagrams (a) and (c), and $M' = M_h$ for diagrams (b) and (d). The ω_i are coefficients that come from the sum over quark color-spin-flavor indices and combinatorial factors, whose values for the $\bar{D}N$ interaction are given in Table 3 of Ref. [13]. The corresponding coefficients for the KN reaction can be extracted from that table by identifying \bar{D}^0 with K^+ and D^- with K^0 . Note that $V_{MB}(\mathbf{p}, \mathbf{p}')$ is symmetric under interchange of \mathbf{p} and \mathbf{p}' and therefore possess post-prior symmetry [67,73], a feature that is not always satisfied when using composite wave functions that are not exact eigenstates of the microscopic Hamiltonian [74]. As mentioned earlier, the quark-interchange mechanism leads to an effective meson-baryon potential that is of very short range. It depends on the overlap of the hadron wave functions and contributes mostly to s waves. As shown in Ref. [23], in order to describe experimental data for the K^+N and K^0N reactions, light-meson exchange processes are required to account for medium- and long-ranged components of the force. Quark interchange generated by OGE accounts roughly for only 50% of the experimental s -wave phase shifts; vector- (ω and ρ) and scalar-meson exchanges are crucial for the correct description of this wave and higher partial waves as well [23]. Moreover, in order to describe the correct isospin dependence of the data, it is essential to include the exchange of the scalar-isovector a_0 meson [23]. With these facts in mind, we follow Ref. [13] and include meson-exchanges in the $\bar{D}N$ system. As in that reference, we parametrize correlated $\pi\pi$ exchange in terms of a single σ -meson exchange: This is not a bad approximation for the $I = 0$ channel, but for $I = 1$ channel it underestimates the total strength by 50% [13]. In Appendix we present the effective Lagrangians densities and corresponding one-meson-exchange amplitudes.

IV. NUMERICAL RESULTS FOR PHASE SHIFTS AND CROSS SECTIONS

As mentioned previously, not much is known experimentally about the $\bar{D}N$ interaction at low energies. In view of this, and in order to have a comparison standard, we

also consider within the same model, without changing any parameters besides the current quark masses, the K^+N and K^0N elastic processes, for which there are experimental data. It is important to reiterate that the effective short-range meson-baryon potential derived from quark-interchange driven by the microscopic interactions of model 1 or model 2 are very constrained, in the sense that they are determined by the microscopic interactions V_C and D_T via a chain of intermediate results for hadron properties driven by $D\chi$ SB. That is, the microscopic interactions V_C and D_T determine the constituent quark masses $M_l = (M_u, M_d)$ and $M_h = (M_s, M_c)$, and these quark masses together with V_C and D_T determine the hadron wave functions. The effective meson-baryon interaction is determined by all these ingredients simultaneously, since it depends explicitly on the hadron wave functions, the quark masses, and V_C and D_T . Such an interdependent chain of results determining the effective meson-baryon interaction is absent in the NRQM with OGE, where quark masses are independent of the microscopic quark-antiquark Hamiltonian.

Having determined the constituent quark masses $M_l = (M_u, M_d)$ and $M_h = (M_s, M_c)$, the next step is the determination of the variational parameters α and β of the ψ and ϕ wave functions. Minimization of M_N and M_P with respect to α and β leads to the results shown in Table I; also shown are the parameters used with the OGE model in Refs. [13,23].

As expected, because the charm quark is heavier than the strange quark, the charmed D mesons are smaller objects than the kaons; recall that the meson root mean square radii are inversely proportional to β . One also sees that hadron sizes of models 1 and 2 are smaller than those used in the OGE model. Although the sizes of the wave functions have an influence on the degree of overlap of the colliding hadrons, the microscopic interactions V_C and D_T also play roles in the effective meson-baryon potentials. As we discuss shortly, there is an interesting interplay between these two effects. For a recent discussion on the influence of hadron sizes on the quark-interchange mechanism, see Ref. [75]. Regarding the hadron masses, one sees a discrepancy of 25% (model 1) and 50% (model 2) on the kaon-nucleon mass difference; this does not come as a surprise in view of the pseudo-Goldstone boson nature of the kaon, in that a BCS variational form for the kaon wave function is a poor substitute for the full Salpeter amplitude [51,52]. On the other hand, the DN mass difference is within 10% of the experimental value in both model 1 and model 2.

We are now in position to discuss numerical results for scattering observables. We solve numerically the Lippmann-Schwinger equation for the potentials derived from the quark-interchange mechanism and one-meson exchanges, using the method discussed in Sec. 2.4 of Ref. [76]. The importance of going beyond quark-Born diagrams by iterating the quark-interchange potentials in a scattering equation has been stressed previously [13,23,68]. For the specific case of the OGE quark-interchange in $\bar{D}N$ scattering, unitarization of the scattering amplitude by iteration in a Lippmann-Schwinger equation leads to a decrease of the cross section at low energies by a factor of three as compared to the nonunitarized quark-Born amplitude [13].

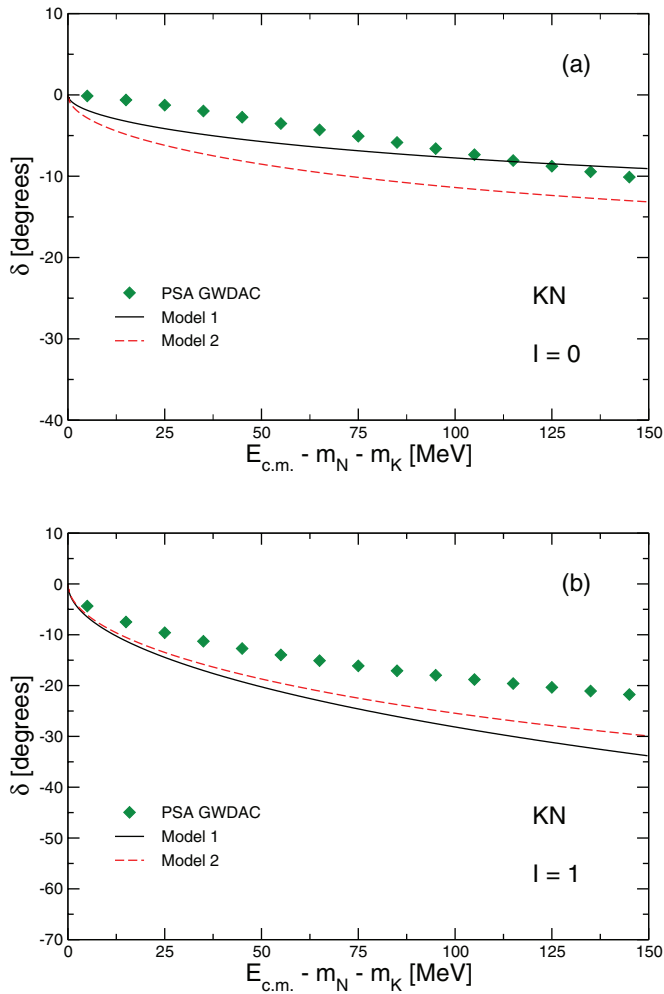


FIG. 3. (Color online) KN s -wave phase shifts for isospin (a) $I = 0$ (upper panel) and (b) $I = 1$ channels from the quark-interchange meson-baryon potential driven by the microscopic interactions of model 1 (solid lines) and model 2 (dashed lines). The curve with diamond symbols and denoted PSA GWDAC are the results from a phase-shift analysis from the George Washington Data Analysis Center (GWDAC), Ref. [77].

In Fig. 3 we present results for the s -wave phase shifts for the isospin $I = 0$ and $I = 1$ of the K^+N and K^0N reactions. Here we show the results derived from the baryon-meson potential obtained from the quark-interchange mechanism driven by the microscopic interactions of model 1 and model 2. Also shown in the figure are results from a phase shift analysis from the George Washington Data Analysis Center (GWDAC) [77]. As in the case of the model with OGE [23], both model 1 and model 2 reproduce the experimental fact that the s -wave phase shifts for $I = 0$ are much smaller than for $I = 1$. This is due to the combined effects that for $I = 0$, the confining interaction V_C does not contribute at all and D_T contributes only via diagrams c and d of Fig. 2.

Also seen in Fig. 3 is the fact that both model 1 and model 2 provide large repulsion: The confining interaction V_C of model 2 provides a little more repulsion than the V_C from model 1. As

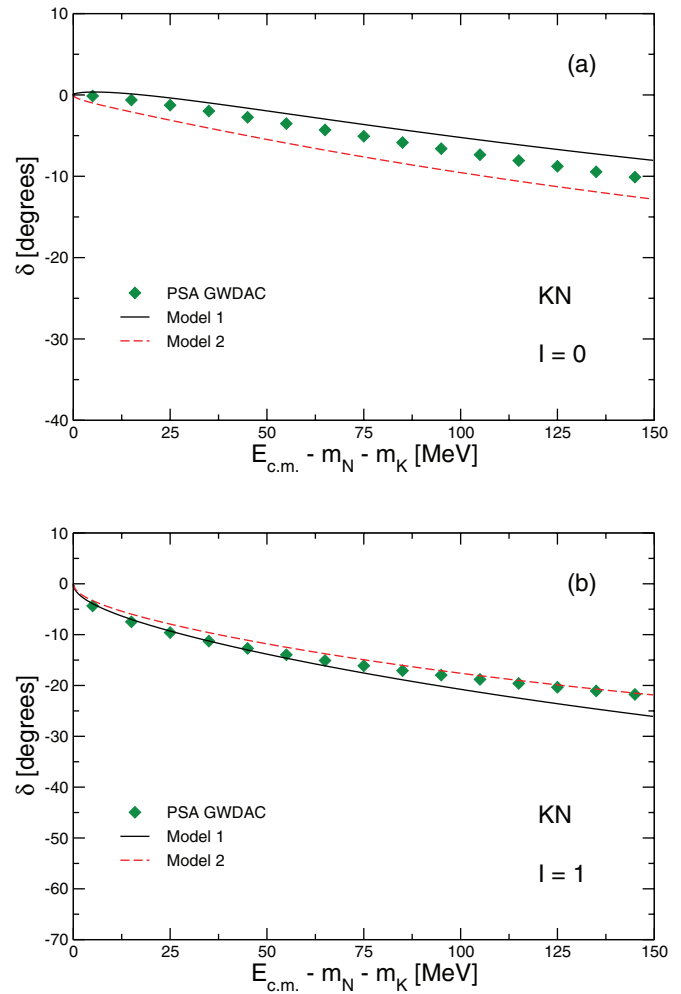


FIG. 4. (Color online) Same as in Fig. 3, but with meson-exchange potentials added to the quark-interchange meson-baryon potential.

in the case of OGE, meson exchanges can be added to obtain a fair description of the data, as we discuss next.

In Fig. 4 we present results for the phase shifts when (σ , ω , ρ , and a_0) one-meson exchanges are added to the quark-interchange potential. The input parameters for the meson-exchange potential are cutoff masses in form factors and coupling constants: We take the values used in Refs. [13,23], with the exception of the σ and a_0 couplings, and the product $g_{\sigma MM}g_{\sigma BB}$ is increased by four and the product $g_{a_0 MM}g_{a_0 BB}$ is increased by three for a reasonable description of the phases. This is because the quark-interchange potential gives strong repulsion. Once the K^+N and K^0N phase shifts are fitted, we use the same values of the cutoff masses and couplings to make predictions for the $\bar{D}N$ system, which we discuss next. We note that through fine tuning of the cutoff masses and further fine adjustments of couplings, the fits in Fig. 4 can be improved. However, for the purposes of the present paper, such a fine adjustment is not important.

In Fig. 5 we present the s -wave phase shifts for isospin $I = 0$ and $I = 1$ states of the \bar{D}^0N and D^-N reactions.

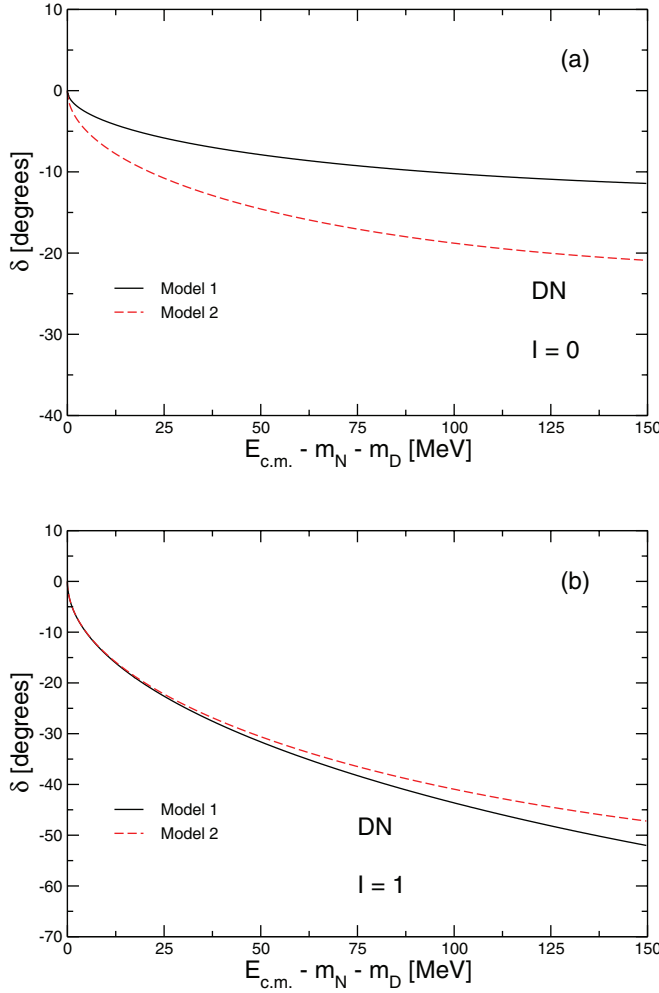


FIG. 5. (Color online) $\bar{D}N$ s -wave phase shifts for (a) $I = 0$ and (b) $I = 1$ channels from the quark-interchange meson-baryon potential driven by the microscopic interactions of model 1 (solid lines) and model 2 (dashed lines).

Results are obtained with a meson-baryon potential from quark-interchange driven by the interactions of model 1 and model 2. Like in the similar KN system, the phases for the $I = 1$ channel are much bigger than those for the $I = 0$ channel. Also, one sees that model 2 gives a stronger repulsion.

Adding (σ , ω , ρ , and a_0) one-meson exchanges to the quark-interchange potential leads to the results shown in Fig. 6. Parameters of the meson-exchange potentials are the same used for the KN . The predictions for the s -wave phase shifts for $\bar{D}N$ system are qualitatively similar to the results for the KN system but are roughly a factor of two larger than the latter ones.

The quark-interchange meson-baryon potential leads to much smaller phase shifts for the higher partial waves. Like in the KN system, meson exchanges play a much more important role in those waves. Although not shown here, many important features of the meson exchanges discussed in Ref. [13], as the interference pattern between ρ and ω contributions (destructive for $I = 0$ and constructive for $I = 1$) are seen in the present

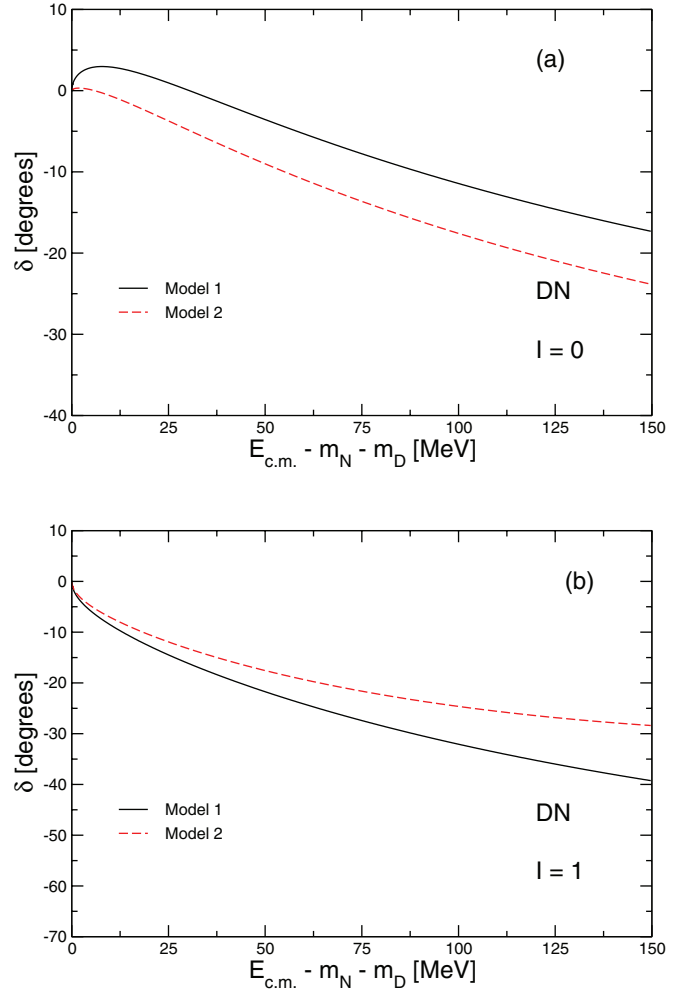


FIG. 6. (Color online) Same as in Fig. 5, but with meson-exchange potentials added to the quark-interchange meson-baryon potential.

model as well. We do not show these detailed results here, as they concern the meson exchange part of the full interaction, but we present in Fig. 7 the final predictions for $\bar{D}N$ cross sections. However, for comparison, we also show in the same figure the corresponding predictions for cross sections of Ref. [13].

The results from both confining models are qualitatively similar, although the results from model 1 for the $I = 1$ state are on average larger by a factor roughly equal to 2. It is important to note that in the present paper we are approximating the correlated two-pion exchange contribution by single σ -meson exchange. As seen in Ref. [13], this seems to be a reasonable approximation for the $I = 0$ channel but underestimates the $I = 1$ cross section by a factor roughly equal to 2; this can be seen in panel (b) of Fig. 7, where the blue (dash-dotted) line is obtained with correlated two-pion exchange while the green (dash-double-dotted) line is obtained with single σ -meson exchange. We expect that a similar feature would be seen with the quark models discussed in the present paper. The corresponding $I = 0$ and $I = 1$ s -wave scattering lengths a_0 and a_1 are for model 1, $a_0 = 0.16$ fm and

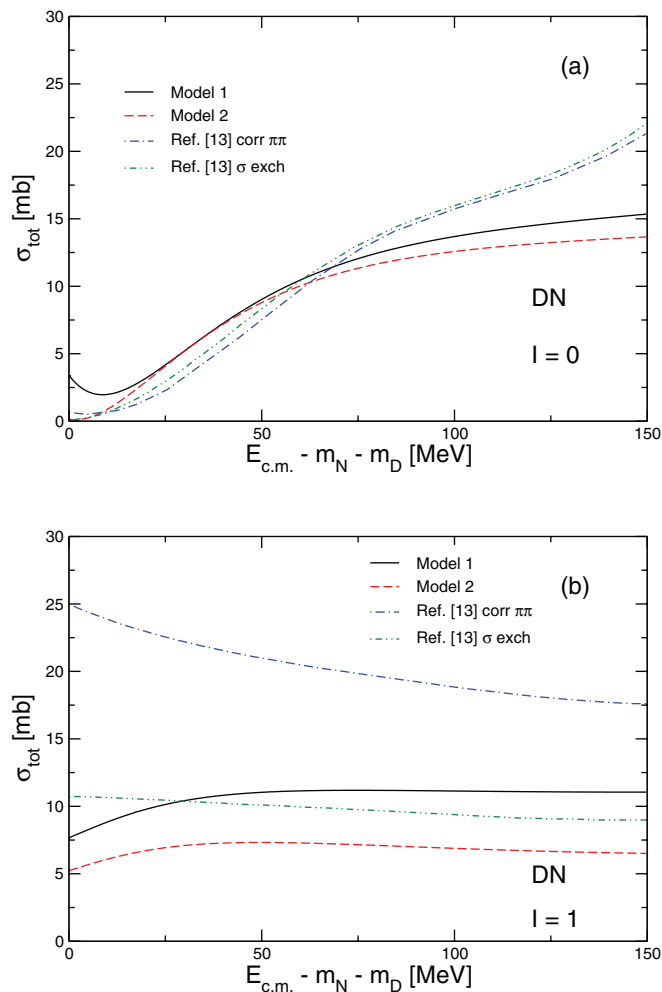


FIG. 7. (Color online) Predictions of $\bar{D}N$ cross sections for (a) $I = 0$ and (b) $I = 1$ using the full meson-baryon potential with quark-interchange and meson exchanges. Also shown are the predictions of Ref. [13].

$a_1 = -0.25$ fm; for model 2, $a_0 = 0.03$ fm and $a_1 = -0.20$ fm [the sign convention is $k \cot \delta = 1/a$]. These values should be contrasted with those of the full model of Ref. [13]: $a_0 = 0.07$ fm and $a_1 = -0.45$ fm.

As a final remark, we note that the results for the cross sections are of the same order of magnitude as those from OGE quark interchange, but the shapes of the curves for the $I = 1$ cross sections from model 1 and model 2 are different at very low energies from those from OGE. This last feature can possibly be attributed to the drastically different momentum dependences of $V_C(k)$ and $V_T(k)$ from the $1/k^2$ dependence of the OGE.

V. CONCLUSIONS AND PERSPECTIVES

There is great contemporary interest in studying the interaction of charmed hadrons with ordinary hadrons and nuclei. Of particular interest is the study of D mesons in medium, mainly in connection with the possibility of creating

new exotic nuclear bound states by nuclei-capturing charmonia states like J/Ψ and η_c [2–5] or D and D^* mesons [6–8]. One major difficulty here is the complete lack of experimental information on the free-space interactions that would be of great help to guide model building; this is not the case for the similar problems involving strange hadrons. In a situation with a lack of experimental information, one way to proceed in model building is to use symmetry constraints, analogies with other similar processes, and different degrees of freedom [13,20–22]. With such a motivation, we have implemented a calculation scheme for deriving effective low-energy hadron-hadron interactions based on a phenomenological Hamiltonian inspired in the QCD Hamiltonian in Coulomb gauge. The model Hamiltonian, defined in Eqs. (1)–(7), confines color and realizes $D\chi$ SB. The scheme makes contact with traditional constituent quark models [33] but it goes beyond such models: The constituent quark masses are derived from the very same interactions that lead to hadron bound states and hadron-hadron interactions, while in the traditional quark models, quark masses and quark-quark interactions are specified independently. Moreover, the model confines color, in that only color-singlet hadron states are of finite energy. These features of the model are essential for studies seeking signals of in-medium modifications of hadron properties.

The model Hamiltonian requires as input a Coulomb-like term V_C and a transverse-gluon interaction D_T . We used two analytical forms for V_C : Model 1 is a parametrization of the lattice simulation of QCD in Coulomb gauge of Ref. [55] and model 2 was used in recent studies of glueballs [56] and heavy hybrid quarkonia [57]. For D_T we were guided by previous studies of spin-hyperfine splittings of meson masses [38]. Initially, we obtained the constituent quark mass function $M_f(k)$ for different flavors f . Next, we derived an effective low-energy meson-baryon interaction from a quark-interchange mechanism, whose input is the microscopic Hamiltonian and hadron bound-state wave functions given in terms of quark degrees of freedom [67,68]. We derived explicit analytical expressions for the effective meson-baryon interaction by using a low-momentum expansion of the constituent quark mass function and variational hadron wave functions [47,51]. Initially we used the short-ranged quark-interchange potential derived within the model and added one-meson-exchange potentials to fit experimental s -wave phase shifts of the K^+N and K^0N reactions. Next, without changing any parameters besides the strange to charm current quark masses, $m_s \rightarrow m_c$, we presented the predictions of the model for the \bar{D}^0N and D^-N reactions. The results for the cross sections obtained with the present model are of the same order of magnitude as those from OGE quark interchange, of the order of 5 mb for the $I = 1$ state and 10 mb for the $I = 0$ state, on average. However, the shapes of the curves for the $I = 1$ cross sections from model 1 and model 2 are different at very low energies from those from OGE, a feature we attribute to the drastically different momentum dependences of $V_C(k)$ and $V_T(k)$ from the $1/k^2$ dependence of the OGE.

The model can be improved in several directions. First of all, without sacrificing the ability to obtain analytical expressions for the effective meson-baryon interaction, one can expand the amplitudes ψ and ϕ in a basis of several Gaussians

and diagonalize the resulting Hamiltonian matrix together with a variational determination of the size parameters of the Gaussians. Another improvement that certainly will be necessary for studying in-medium chiral symmetry restoration is to use the full mass function $M_f(k)$ for the light u and d flavors, instead of the low-momentum expansion of Eq. (32). This is because at finite baryon density and/or temperature, the mass function $M_f(k)$ for $f = (u, d)$ loses strength in the infrared [45,78–81] and the expansion in powers of k^2/M^2 evidently loses validity. However, this will have a slight impact on the numerics, since in this case multidimensional integrals for the determination of the hadron sizes and the effective meson-baryon interaction need to be performed numerically. The low-momentum expansion must also be abandoned in the calculation of hadron wave functions when the quark mass function $M_f(k)$ in the infrared is much smaller than the average momentum of the quark in the hadron. Such a situation can happen when $D_T(k)$ is suppressed in the infrared, as in the study of Ref. [65].

Finally, another subject that needs careful scrutiny is the use of SU(4) flavor symmetry, Eq. (A10), to fix the coupling constants in the effective meson Lagrangians. A recent estimation [82], using a framework in which quark propagators and hadron amplitudes are constrained by Dyson-Schwinger equation studies in QCD, finds that while SU(3) flavor symmetry is accurate to 20%, SU(4) relations underestimate the $DD\rho$ coupling by a factor of 5. On the other hand, a study employing a 3P_0 pair-creation model with nonrelativistic quark model hadron wave functions finds smaller SU(4) breakings [83]. In addition, one should note that use of the vector-meson dominance hypothesis to the process $e^-D^+ \rightarrow e^-D^+$ leads to a value for the $g_{DD\rho}$ coupling which is very close to the SU(4) symmetry prediction [84].

ACKNOWLEDGMENTS

This work was partially funded by Conselho Nacional de Desenvolvimento Científico e Tecnológico (Brazil’s National Council of Technological and Scientific Development) and Fundação de Amparo à Pesquisa do Estado de São Paulo (Foundation for Research Support of the State of São Paulo).

APPENDIX: MESON-EXCHANGE CONTRIBUTIONS

The meson-exchange contributions are obtained from the following effective Lagrangian densities [84,85]:

$$\mathcal{L}_{NNS}(x) = g_{NNS} \bar{\psi}^{(N)}(x) \boldsymbol{\tau} \cdot \boldsymbol{\phi}^{(S)}(x) \psi^{(N)}(x), \quad (\text{A1})$$

$$\begin{aligned} \mathcal{L}_{NNV}(x) = & g_{NNV} \left[\bar{\psi}^{(N)}(x) \gamma^\mu \psi^{(N)}(x) \boldsymbol{\tau} \cdot \boldsymbol{\phi}_\mu^{(V)}(x) \right. \\ & \left. + \left(\frac{\kappa_V}{2M_N} \right) \bar{\psi}^{(N)}(x) \sigma^{\mu\nu} \psi^{(N)}(x) \boldsymbol{\tau} \cdot \partial_\nu \boldsymbol{\phi}_\mu^{(V)}(x) \right], \end{aligned} \quad (\text{A2})$$

$$\mathcal{L}_{PPS}(x) = g_{PPS} \varphi^{(P)}(x) \phi^{(S)}(x) \varphi^{(P)}(x), \quad (\text{A3})$$

$$\mathcal{L}_{PPV}(x) = i g_{PPV} \left[\varphi^{(P)}(x) (\partial_\nu \varphi^{(P)}(x)) \boldsymbol{\tau} \right. \\ \left. - (\partial_\nu \varphi^{(P)}(x)) \boldsymbol{\tau} \varphi^{(P)}(x) \right] \cdot \boldsymbol{\phi}_\nu^{(V)}(x). \quad (\text{A4})$$

In these, $\psi^{(N)}$ denotes the nucleon doublet, $\phi^{(P)}(x)$ is the charmed and strange meson doublet, $\boldsymbol{\phi}_\mu^{(V)}(x)$ is the isotriplet of ρ mesons, and $\boldsymbol{\tau}$ are the Pauli matrices. The Lagrangians for the σ and ω mesons are obtained by taking $\boldsymbol{\tau} \rightarrow 1$ in the expressions above and in addition $\kappa_V = 0$ for the case of ω .

The tree-level potentials derived from the above Lagrangian densities lead to the following expressions for the vector-meson exchanges ($v = \rho, \omega$):

$$\begin{aligned} V^v(\mathbf{p}, \mathbf{p}') = & \frac{g_{NNv} g_{PPv}}{(2\pi)^3 \sqrt{4\omega(p)\omega(p')}} (p' + p)_\mu \Delta_v^{\mu\nu}(q) \\ & \times \left[A_v(pS, p's') + \left(\frac{\kappa_v}{2m_N} \right) B_v(pS, p's') \right]. \end{aligned} \quad (\text{A5})$$

For the scalar-meson exchanges ($S = \sigma, a_0$),

$$V^S(\mathbf{p}', \mathbf{p}) = \frac{g_{NNS} g_{PPS}}{(2\pi)^3 \sqrt{4\omega(p)\omega(p')}} \Delta_S(q) \bar{u}(\mathbf{p}', s') u(\mathbf{p}, s), \quad (\text{A6})$$

where m_N is the nucleon mass and $\omega(q) = (q^2 + m^2)^{1/2}$ with m the meson masses, $\Delta_v^{\mu\nu}(q)$ and $\Delta_S(q)$ are the vector-meson and scalar-meson propagators, $u(\mathbf{p}, s)$ are the Dirac spinors of nucleons [same expression as in Eq. (9), with $M(k)$ replaced by the nucleon mass m_N], and the quantities A_μ and B_μ are given by

$$A_\mu(pS, p's') = \bar{u}(\mathbf{p}', s') \gamma_\mu u(\mathbf{p}, s), \quad (\text{A7})$$

$$B_\mu(pS, p's') = \bar{u}(\mathbf{p}', s') i \sigma_{\mu\nu} q^\nu u(\mathbf{p}, s). \quad (\text{A8})$$

To avoid divergences in the Lippmann-Schwinger equation, the meson-exchange potentials are regularized phenomenologically by monopole form factors at each vertex:

$$F_i(q^2) = \left(\frac{\Lambda_i^2 - m_i^2}{\Lambda_i^2 + q^2} \right), \quad (\text{A9})$$

where $\mathbf{q} = \mathbf{p}' - \mathbf{p}$, m_i is the mass of the exchanged meson and Λ_i is a cutoff mass. The coupling constants are fixed by SU(4) symmetry as in Ref. [13]:

$$g_{\bar{D}D\rho} = g_{\bar{D}D\omega} = g_{KK\rho} = g_{KK\omega} = \frac{g_{\pi\pi\rho}}{2}. \quad (\text{A10})$$

[1] R. Rapp, D. Blaschke, and P. Crochet, *Prog. Part. Nucl. Phys.* **65**, 209 (2010).
 [2] S. J. Brodsky, I. A. Schmidt, and G. F. de Teramond, *Phys. Rev. Lett.* **64**, 1011 (1990).

[3] S. H. Lee and C. M. Ko, *Phys. Rev. C* **67**, 038202 (2003).
 [4] G. Krein, A. W. Thomas, and K. Tsushima, *Phys. Lett. B* **697**, 136 (2011).

- [5] K. Tsushima, D. H. Lu, G. Krein, and A. W. Thomas, *Phys. Rev. C* **83**, 065208 (2011).
- [6] K. Tsushima, D. H. Lu, A. W. Thomas, K. Saito, and R. H. Landau, *Phys. Rev. C* **59**, 2824 (1999).
- [7] C. Garcia-Recio, J. Nieves, and L. Tolos, *Phys. Lett. B* **690**, 369 (2010).
- [8] C. Garcia-Recio, J. Nieves, L. L. Salcedo, and L. Tolos, *Phys. Rev. C* **85**, 025203 (2012).
- [9] R. S. Hayano and T. Hatsuda, *Rev. Mod. Phys.* **82**, 2949 (2010).
- [10] T. Mizutani and A. Ramos, *Phys. Rev. C* **74**, 065201 (2006).
- [11] Z.-w. Lin, C. M. Ko, and B. Zhang, *Phys. Rev. C* **61**, 024904 (2000).
- [12] J. Hofmann and M. F. M. Lutz, *Nucl. Phys. A* **763**, 90 (2005).
- [13] J. Haidenbauer, G. Krein, U.-G. Meißner, and A. Sibirtsev, *Eur. Phys. J. A* **33**, 107 (2007).
- [14] S. Yasui and K. Sudoh, *Phys. Rev. D* **80**, 034008 (2009).
- [15] C. Garcia-Recio, V. K. Magas, T. Mizutani, J. Nieves, A. Ramos, L. L. Salcedo, and L. Tolos, *Phys. Rev. D* **79**, 054004 (2009).
- [16] T. F. Carames and A. Valcarce, *Phys. Rev. D* **85**, 094017 (2012).
- [17] K. Yokokawa, S. Sasaki, T. Hatsuda, and A. Hayashigaki, *Phys. Rev. D* **74**, 034504 (2006).
- [18] T. Kawanai and S. Sasaki, *Phys. Rev. D* **82**, 091501 (2010).
- [19] L. Liu, H.-W. Lin, and K. Orginos, *PoS LATTICE* **2008**, 122 (2008).
- [20] J. Haidenbauer, G. Krein, U.-G. Meißner, and A. Sibirtsev, *Eur. Phys. J. A* **37**, 55 (2008).
- [21] J. Haidenbauer and G. Krein, *Phys. Lett. B* **687**, 314 (2010).
- [22] J. Haidenbauer, G. Krein, U.-G. Meißner, and L. Tolos, *Eur. Phys. J. A* **47**, 18 (2011).
- [23] D. Hadjimichef, J. Haidenbauer, and G. Krein, *Phys. Rev. C* **66**, 055214 (2002).
- [24] R. Büttgen, K. Holinde, A. Müller-Groeling, J. Speth, and P. Wyborny, *Nucl. Phys. A* **506**, 586 (1990).
- [25] M. Hoffmann, J. W. Durso, K. Holinde, B. C. Pearce, and J. Speth, *Nucl. Phys. A* **593**, 341 (1995).
- [26] T. Barnes and E. S. Swanson, *Phys. Rev. C* **49**, 1166 (1994).
- [27] B. Silvestre-Brac, J. Leandri, and J. Labarsouque, *Nucl. Phys. A* **589**, 585 (1995).
- [28] B. Silvestre-Brac, J. Labarsouque, and J. Leandri, *Nucl. Phys. A* **613**, 342 (1997).
- [29] S. Lemaire, J. Labarsouque, and B. Silvestre-Brac, *Nucl. Phys. A* **696**, 497 (2001).
- [30] S. Lemaire, J. Labarsouque, and B. Silvestre-Brac, *Nucl. Phys. A* **700**, 330 (2002).
- [31] S. Lemaire, J. Labarsouque, and B. Silvestre-Brac, *Nucl. Phys. A* **714**, 265 (2003).
- [32] J. Haidenbauer and G. Krein, *Phys. Rev. C* **68**, 052201 (2003).
- [33] F. E. Close, *An Introduction to Quarks and Partons* (Academic Press, New York, 1979).
- [34] E. M. Henley and G. Krein, *Phys. Rev. Lett.* **62**, 2586 (1989).
- [35] E. M. Henley and G. Krein, *Phys. Lett. B* **231**, 213 (1989).
- [36] A. P. Szczepaniak and E. S. Swanson, *Phys. Rev. Lett.* **87**, 072001 (2001).
- [37] A. P. Szczepaniak and E. S. Swanson, *Phys. Rev. D* **65**, 025012 (2001).
- [38] F. J. Llanes-Estrada, S. R. Cotanch, A. P. Szczepaniak, and E. S. Swanson, *Phys. Rev. C* **70**, 035202 (2004).
- [39] P. Bicudo, J. E. Ribeiro, and J. Rodrigues, *Phys. Rev. C* **52**, 2144 (1995).
- [40] J. R. Finger and J. E. Mandula, *Nucl. Phys. B* **199**, 168 (1982).
- [41] A. Amer, A. Le Yaouanc, L. Oliver, O. Pene, and J. C. Raynal, *Phys. Rev. Lett.* **50**, 87 (1983).
- [42] A. Le Yaouanc, L. Oliver, O. Pene, and J. C. Raynal, *Phys. Lett. B* **134**, 249 (1984).
- [43] A. Le Yaouanc, L. Oliver, O. Pene, and J. C. Raynal, *Phys. Rev. D* **29**, 1233 (1984).
- [44] S. L. Adler and A. C. Davis, *Nucl. Phys. B* **244**, 469 (1984).
- [45] A. Kocic, *Phys. Rev. D* **33**, 1785 (1986).
- [46] P. J. d. A. Bicudo and J. E. F. T. Ribeiro, *Phys. Rev. D* **42**, 1611 (1990); **42**, 1625 (1990); **42**, 1635 (1990).
- [47] P. J. A. Bicudo, G. Krein, J. E. F. T. Ribeiro, and J. E. Villate, *Phys. Rev. D* **45**, 1673 (1992).
- [48] H. Mishra and S. P. Misra, *Phys. Rev. D* **48**, 5376 (1993).
- [49] A. Mishra, H. Mishra, V. Sheel, S. P. Misra, and P. K. Panda, *Int. J. Mod. Phys. E* **5**, 93 (1996).
- [50] F. J. Llanes-Estrada and S. R. Cotanch, *Phys. Rev. Lett.* **84**, 1102 (2000).
- [51] P. J. A. Bicudo, G. Krein, and J. E. F. T. Ribeiro, *Phys. Rev. C* **64**, 025202 (2001).
- [52] F. J. Llanes-Estrada and S. R. Cotanch, *Nucl. Phys. A* **697**, 303 (2002).
- [53] N. Ligterink and E. S. Swanson, *Phys. Rev. C* **69**, 025204 (2004).
- [54] R. F. Wagenbrunn and L. Y. Glozman, *Phys. Rev. D* **75**, 036007 (2007).
- [55] A. Voigt, E.-M. Ilgenfritz, M. Müller-Preussker, and A. Sternbeck, *Phys. Rev. D* **78**, 014501 (2008).
- [56] P. Guo, A. P. Szczepaniak, G. Galata, A. Vassallo, and E. Santopinto, *Phys. Rev. D* **77**, 056005 (2008).
- [57] P. Guo, A. P. Szczepaniak, G. Galata, A. Vassallo, and E. Santopinto, *Phys. Rev. D* **78**, 056003 (2008).
- [58] Y. Nakagawa, A. Voigt, E.-M. Ilgenfritz, M. Müller-Preussker, A. Nakamura, T. Saito, A. Sternbeck, and H. Toki, *Phys. Rev. D* **79**, 114504 (2009).
- [59] R. Alkofer, M. Kloker, A. Krassnigg, and R. F. Wagenbrunn, *Phys. Rev. Lett.* **96**, 022001 (2006).
- [60] A. P. Szczepaniak (private communication).
- [61] T. Nguyen, N. A. Souchlas, and P. C. Tandy, *AIP Conf. Proc.* **1361**, 142 (2011).
- [62] C. D. Roberts, M. S. Bhagwat, A. Holl, and S. V. Wright, *Eur. Phys. J. ST* **140**, 53 (2007).
- [63] R. Alkofer, W. Detmold, C. S. Fischer, and P. Maris, *Phys. Rev. D* **70**, 014014 (2004).
- [64] V. N. Gribov, *Nucl. Phys. B* **139**, 1 (1978).
- [65] M. Pak and H. Reinhardt, *Phys. Lett. B* **707**, 566 (2012).
- [66] F. Myhrer and J. Wroldsen, *Rev. Mod. Phys.* **60**, 629 (1988).
- [67] D. Hadjimichef, G. Krein, S. Szpigel, and J. S. da Veiga, *Ann. Phys.* **268**, 105 (1998).
- [68] D. Hadjimichef, J. Haidenbauer, and G. Krein, *Phys. Rev. C* **63**, 035204 (2001).
- [69] A. De Rujula, H. Georgi, and S. L. Glashow, *Phys. Rev. D* **12**, 147 (1975).
- [70] L. McLerran and R. D. Pisarski, *Nucl. Phys. A* **796**, 83 (2007).
- [71] L. Y. Glozman, *Phys. Rev. D* **79**, 037504 (2009).
- [72] L. Y. Glozman, *Phys. Rev. D* **80**, 037701 (2009).
- [73] C.-Y. Wong, E. S. Swanson, and T. Barnes, *Phys. Rev. C* **62**, 045201 (2000).
- [74] L. I. Schiff, *Quantum Mechanics* (McGraw-Hill, New York, 1968), pp. 384–387.
- [75] J. Vijande, G. Krein, and A. Valcarce, *Eur. Phys. J. A* **40**, 89 (2009).

- [76] S. K. Adhikari, *Variational Principles and the Numerical Solution of Scattering Problems* (Wiley, New York, 1998).
- [77] CNS DAC Services [<http://gwdac.phys.gwu.edu>].
- [78] A. C. Davis and A. M. Matheson, *Nucl. Phys. B* **246**, 203 (1984).
- [79] R. Alkofer, P. A. Amundsen, and K. Langfeld, *Z. Phys. C* **42**, 199 (1989).
- [80] P. Guo and A. P. Szczepaniak, *Phys. Rev. D* **79**, 116006 (2009).
- [81] P. M. Lo and E. S. Swanson, *Phys. Rev. D* **81**, 034030 (2010).
- [82] B. El-Bennich, G. Krein, L. Chang, C. D. Roberts, and D. J. Wilson, *Phys. Rev. D* **85**, 031502 (2012).
- [83] C. E. Fontoura, J. Haidenbauer, and G. Krein (unpublished).
- [84] Z.-w. Lin and C. M. Ko, *Phys. Rev. C* **62**, 034903 (2000).
- [85] Z.-w. Lin, T. G. Di, and C. M. Ko, *Nucl. Phys. A* **689**, 965 (2001).